Journal of Biomolecular NMR, 9 (1997) 273–286
ESCOM

J-Bio NMR 426

NMR secondary structure of the plasminogen activator protein staphylokinase

O. Ohlenschläger[a], R. Ramachandran[a], J. Flemming[a], K.-H. Gührs[b], B. Schlott[b] and L.R. Brown[a,*]

Departments of [a]Molecular Biophysics/NMR Spectroscopy and [b]Biochemistry, Institute of Molecular Biotechnology, P.O. Box 100813, D-07708 Jena, Germany

Received 23 October 1996
Accepted 20 December 1996

Keywords: Secondary structure; NOE; Chemical shift; Heteronuclear NMR; Staphylokinase; Plasminogen; Resonance assignment

Summary

Staphylokinase (Sak) is a 15.5 kDa protein secreted by several strains of *Staphylococcus aureus*. Due to its ability to convert plasminogen, the inactive proenzyme of the fibrinolytic system, into plasmin, Sak is presently undergoing clinical trials for blood clot lysis in the treatment of thrombovascular disorders. With a view to developing a better understanding of the mode of action of Sak, we have initiated a structural investigation of Sak via multidimensional heteronuclear NMR spectroscopy employing uniformly ^{15}N- and ^{15}N,^{13}C-labelled Sak. Sequence-specific resonance assignments have been made employing ^{15}N-edited TOCSY and NOE experiments and from HNCACB, CBCA(CO)NH, HBHA-(CBCACO)NH and CC(CO)NH sets of experiments. From an analysis of the chemical shifts, $^{3}J_{H^{N}H^{\alpha}}$ scalar coupling constants, NOEs and H^{N} exchange data, the secondary structural elements of Sak have been characterized.

Introduction

Staphylokinase (Sak) is a protein secreted by several strains of *Staphylococcus aureus* and is capable of converting the human plasma zymogen plasminogen (Plg) into the protease plasmin (Pli). The main function of plasmin is the proteolytic degradation of fibrin, which is the major noncellular component of blood clots. Therefore, Sak is a potential candidate for the lysis of blood clots in the treatment of thrombovascular disorders. The results of clinical trials using recombinant Sak for lytic therapy of myocardial infarction (Collen and Van de Werf, 1993) and peripheral thrombosis (Vanderschueren et al., 1995) fulfil these expectations. Despite the lack of specific fibrin binding sites, i.e. the lysine binding sites located in the kringle domains of the endogenous plasminogen activators t-PA and urokinase normally present in human plasma, Sak expresses a fibrin-specific mode of action. Sak needs at least catalytic amounts of Pli for activating plasminogen (Lijnen et al., 1991; Collen et al., 1993). Therefore, traces of Pli, available in vivo only in the microenvironment of blood clots, induce the process of plasminogen activation by Sak in proximity to these clots. This drastically reduces the risk of systemic disbalancing of the endogenous fibrinolytic system. This feature together with the effective control of the activator species by the endogenous plasmin inhibitor α2-antiplasmin in the absence of fibrin (Lijnen et al., 1991; Silence et al., 1993) results in a degree of fibrin specificity of Sak comparable to that of the endogenous activators. In contrast to t-PA and urokinase, Sak lacks any detectable proteolytic activity. The plasminogen activator species is presently characterized as a Pli–Sak complex generated by intramolecular conversion(s) from an initially formed inactive Plg–Sak complex (Collen et al., 1993). Presumably, the proteolytic function results from the Pli part of the complex. However, Pli itself is not able to cleave the 'activation' Arg^{561}–Val^{562} peptide bond in plasminogen yielding the two chain Pli. Therefore, it is assumed that complex formation with Sak alters the enzymatic specificity of Pli.

*To whom correspondence should be addressed.

Abbreviations: CSI, chemical shift index; EDTA, ethylenediaminetetraacetic acid; EGTA, ethylene glycol-bis(β-aminoethyl ether) *N*,*N*,*N*′,*N*′-tetraacetic acid; IPTG, isopropyl β-D-thiogalactopyranoside; PMSF, phenylmethylsulfonyl fluoride; Sak, staphylokinase; TLCK, Na-*p*-tosyl-L-lysine chloromethyl ketone; TPCK, *N*-tosyl-L-phenylalanine chloromethyl ketone; Plg, plasminogen; Pli, plasmin.

To characterize structure–function relationships, we have recently undertaken an NMR study of Sak, and in the present paper we report initial results carried out employing ^{15}N-labelled and ^{13}C,^{15}N-labelled samples of Sak. Secondary structure elements have been characterized by chemical shift index (CSI), J coupling data, H/D exchange and NOE measurements.

Materials and Methods

Protein expression, purification and NMR sample preparation

The wild-type staphylokinase SakSTAR (Collen et al., 1992) was expressed in *E. coli* TG1 transformed with plasmid pMEX602SakB as recently described (Schlott et al., 1994b). Separate fermentations were performed under vigorous shaking at 37 °C in culture flasks containing 200 or 250 ml synthetic medium (containing 50 μg ml^{-1} ampicillin (Roth, Karlsruhe, Germany)) complemented with $^{15}NH_4Cl$ and glucose or $^{15}NH_4Cl$ and ^{13}C-glucose (Isotec, Miamisburg, OH, U.S.A.), respectively. Expression of the recombinant protein was induced by addition of IPTG (BIOMOL, Hamburg, Germany) to a concentration of 0.2 mM when the cultures reached $OD_{550} = 0.4$. Shaking was continued for 7 h, reaching a final density of cells of $OD_{550} = 2.2$. The bacteria were harvested by centrifugation and washed with 0.9% NaCl and finally the pellets were stored at –20 °C until sonication. Cell disruption was accomplished by three cycles of 5 min of controlled sonication at 0–4 °C in disruption buffer (40 mM potassium phosphate, 10 mM EDTA, 10 mM EGTA, 30 mM NaCl, 10 mM 2-mercaptoethanol, pH 8.0) containing 4 mM PMSF. EDTA, EGTA, TLCK, TPCK and buffer salts were supplied by Sigma (Deisenhofen, Germany) and PMSF by Roth.

Purification of the overexpressed protein was performed by a combination of cation exchange chromatography and subsequent hydrophobic interaction chromatography as described previously (Schlott et al., 1994b). The homogeneity of the fractions was verified by electrophoresis in 15% polyacrylamide gels containing SDS. The peak fractions used for further preparation exhibited a single band even when large amounts of protein were applied to the gel lanes.

The homogeneous peak fractions were combined (30 ml containing 23 mg SakSTAR) and PMSF (final concentration 2 mM), EDTA (final concentration 10 mM) and 2-mercaptoethanol (final concentration 1 mM) were added. The sample was concentrated by ultrafiltration using a stirred cell model 8050 (Amicon, Witten, Germany) equipped with a PM10 membrane (Amicon) to a volume of 5 ml. The sample was further concentrated by ultrafiltration using Centricon-10 units (Amicon) to a final volume of 1.2 ml. TPCK and TLCK were added to a final concentration of 1 mM and the sample was incubated for 15 min at room temperature. Afterwards the sample was immediately applied to a NAP-25 column (Pharmacia, Freiburg, Germany) preequilibrated with NMR buffer (50 mM sodium phosphate, pH 6.68, 100 mM NaCl, 1 mM 2-mercaptoethanol, 0.1 mM EDTA) and eluted using the same buffer. The fractions containing the sample were combined and concentrated in a Centricon-10 to a final volume of 400 μl. After adding 35 μl of D_2O (Promochem, Wesel, Germany), the sample was diluted to 600 μl with NMR buffer and filtered through a sterile 0.2 μm filter directly into a sealable NMR tube. After flushing with sterilized argon, the sample was sealed. The concentrations of homogeneous SakSTAR preparations were determined by spectrophotometric detection at 280 nm using an absorption coefficient of 1.1 l g^{-1} cm^{-1}. The final samples had concentrations of 1.1 mM (^{15}N SakSTAR) and 1.28 mM (^{13}C,^{15}N SakSTAR) and exhibited a single protein band in SDS-PAGE.

NMR spectroscopy

All NMR spectra were recorded at 300 K on a Varian INOVA 750 MHz four-channel NMR spectrometer equipped with pulse field gradient accessories and a triple-resonance probe with an actively shielded Z gradient coil. Quadrature detection in the indirect dimensions was achieved via the States procedure (States et al., 1982). Water suppression was achieved via the WATERGATE technique (Piotto et al., 1992) or by low-power presaturation during the recycle delay. ^{15}N and ^{13}C broadband decoupling was accomplished using the GARP (Shaka et al., 1985) or MPF7 (Fujiwara et al., 1993) decoupling schemes. Where applicable, isotropic mixing was effected with either the DIPSI-2 or DIPSI-3 sequences (Shaka et al., 1988). Multidimensional spectral data sets were analyzed with the program XEASY (Bartels et al., 1995) on Silicon Graphics INDY and INDIGO2 workstations. Proton chemical shifts were referenced to the H_2O signal at 4.74 ppm relative to DSS, and ^{15}N chemical shifts were referenced to external 2.9 M $^{15}NH_4Cl$ in 1 M HCl at 24.93 ppm relative to liquid ammonia. ^{13}C chemical shifts were referenced to external dioxane/H_2O at 67.8 ppm (a correction of +1.6 ppm was considered when establishing the CSI charts (Wishart and Sykes, 1994)). Unless indicated, the ^{1}H and ^{15}N carriers were set at 4.74 ppm and 119.5 ppm, respectively, and a recycle time of 1 s was normally employed. Other relevant experimental data acquisition parameters employed in this work are indicated in Table 1.

^{15}N-edited TOCSY-HSQC (Marion et al., 1989) experiments were carried out employing the DIPSI-3 mixing scheme, for mixing times of 26.5 and 53.0 ms. A ^{15}N-edited clean TOCSY experiment was also carried out employing the DIPSI-2 scheme, with a mixing time of 25 ms. In these experiments the ^{1}H carrier was positioned at 6.8 ppm during the TOCSY period and switched back to

TABLE 1
ACQUISITION PARAMETERS FOR THE NMR EXPERIMENTS

Dimensions, experiment	Scans	ω_1 (Hz), pts	ω_2 (Hz), pts	ω_3 (Hz), pts
^{15}N-^{1}H, HSQC	32	2500, 256	10 000, 2048	–
^{1}H-^{15}N-^{1}H, TOCSY-HSQC	16	9000, 128	2500, 48	10 000, 1024
^{1}H-^{15}N-^{1}H, NOESY-HSQC	12	9000, 128	2500, 32	10 000, 2048
^{15}N-^{13}C-^{1}H, HNCO	16	2250, 40	3000, 48	10 000, 1024
^{15}N-^{1}H-^{1}H, HNHA	32	2500, 30	9000, 80	10 000, 1024
^{15}N-^{13}C-^{1}H, HNCACB	32	2250, 32	12 698, 96	10 000, 1024
^{13}C-^{15}N-^{1}H, CBCA(CO)NH	32	12 698, 96	2250, 32	10 000, 1024
^{1}H-^{15}N-^{1}H, HBHA(CBCACO)NH	32	4500, 72	2250, 32	10 000, 1024
^{13}C-^{15}N-^{1}H, CC(CO)NH	32	13 205, 96	2250, 32	10 000, 1024
^{15}N-^{15}N-^{1}H, HSQC-NOESY-HSQC	24	2500, 36	2500, 36	10 000, 1024
^{1}H-^{13}C-^{1}H, HCCH-TOCSY	8	4500, 96	15 000, 96	10 000, 1024

water at 4.74 ppm. 3D ^{15}N-edited NOESY-HSQC (Fesik and Zuiderweg, 1988; Zuiderweg and Fesik, 1989) and 3D ^{15}N-edited HSQC-NOESY-HSQC experiments were carried out employing a mixing time of 50 and/or 100 ms. 3D HNCO (Kay et al., 1990), HNCACB (Wittekind and Müller, 1993), CBCA(CO)NH (Grzesiek and Bax, 1992), HBHA(CBCACO)NH (Grzesiek and Bax, 1993) and CC(CO)NH experiments (Grzesiek et al., 1993) were carried out on the ^{13}C- and ^{15}N-labelled sample as per the literature, employing the WATERGATE scheme for solvent suppression. A gradient-enhanced 3D HCCH-TOCSY experiment (Kay et al., 1993) employed a CC-TOCSY mixing time of 24 ms with the ^{1}H carrier frequency at 3 ppm initially and switched to the water signal during data acquisition. When required, carbonyl decoupling was achieved by the SEDUCE-1 pulse scheme (McCoy and Müller, 1993). The three-bond coupling constant $^{3}J_{H^{N}H^{\alpha}}$ was extracted from the 3D HNHA spectrum (Vuister and Bax, 1993).

The amide proton exchange rates were measured by passing the ^{15}N-labelled Sak within 5 min over a NAP-25 column (Pharmacia) previously equilibrated with D_2O buffer (see above) and 2D HSQC spectra were recorded (4 scans, 128 transients; Bodenhausen and Ruben, 1980) at approximately 0.5, 1, 2, 2.5, 4, 5.5, 8.5, 12, 18, 24, 48 and 168 h after the H/D exchange was initiated.

Results

Resonance assignment

The ^{15}N-^{1}H HSQC spectrum of Sak (Fig. 1) exhibited 125 well-resolved backbone NH correlations of the 126 that were expected. In addition, five pairs of H-N correlations of the five asparagine side chains resonating in this spectral region could also be identified. Triple-resonance 3D experiments with the uniformly ^{15}N,^{13}C-labelled Sak sample were performed to establish sequential connectivities based on scalar couplings. Typical strip plots of HN-CACB, CBCA(CO)NH and CC(CO)NH spectra linking sequential amino acid residues are shown in Fig. 2. Similarly, Fig. 3 shows typical strip plots of the ^{15}N-edited TOCSY and the HBHA(CBCACO)NH spectra indicating the sequential connectivities seen. By this approach, fragments of 2–21 residues could be linked. These pairs of experiments permitted the unambiguous identification of approximately 85% of the sequential connectivities as well as the characterization of glycine, alanine, serine and threonine residues from the unique C^{α}/C^{β} chemical shifts of these residues. Six of the eight glycines also showed two distinct H^{α} cross peaks in the HSQC-TOCSY. For a given NH of residue i, the possible amino acid types of the preceding residue (i – 1) could be identified in most cases from the specific number of ^{13}C resonances seen in the CC(CO)NH spectrum. Through the identification of intraresidue NOEs involving the backbone and side-chain NHs and the common H^{β} protons, the asparagine backbone NH resonances could be identified. The mapping of the fragments to the amino acid sequence used the information about amino acid type (asparagine, glycine, alanine, serine, threonine) and the number of side-chain carbon atoms of the previous residue. For Sak, whose primary structure is shown in Fig. 5, this procedure allowed sequence-specific assignments to be obtained for the following fragments: Phe^{4}–Gly^{7}, Lys^{8}–Asp^{13}, Asp^{14}–Glu^{19}, Pro–Thr^{21}–Gly^{22}, Thr^{30}–Ser^{34}, Gly^{36}–Ser^{41}, Pro–Gly^{52}–Leu^{55}, Ala^{70}–Tyr^{73}, Pro–Ser^{84}–Phe^{104}, Pro–Ile^{106}–Val^{113}, Asp^{115}–Asn^{122}, Pro–Gly^{124}–Ile^{128}, Thr^{129}–Lys^{136}. For instance, because of the singularity of the Gly^{36}–Asn^{37} sequence a fragment of six residues starting with glycine followed by asparagine could be immediately mapped to amino acids 36–41. The above scalar coupling based experiments also provided three fragments of three sequentially connected residues, three fragments of two sequentially connected residues and one fragment of six residues which did not include asparagine, glycine, alanine, serine or threonine residues. For these fragments, an analysis of the expected and observed numbers of side-chain carbon resonances seen in the CC(CO)NH spectrum allowed the sequence-specific assignment of the following

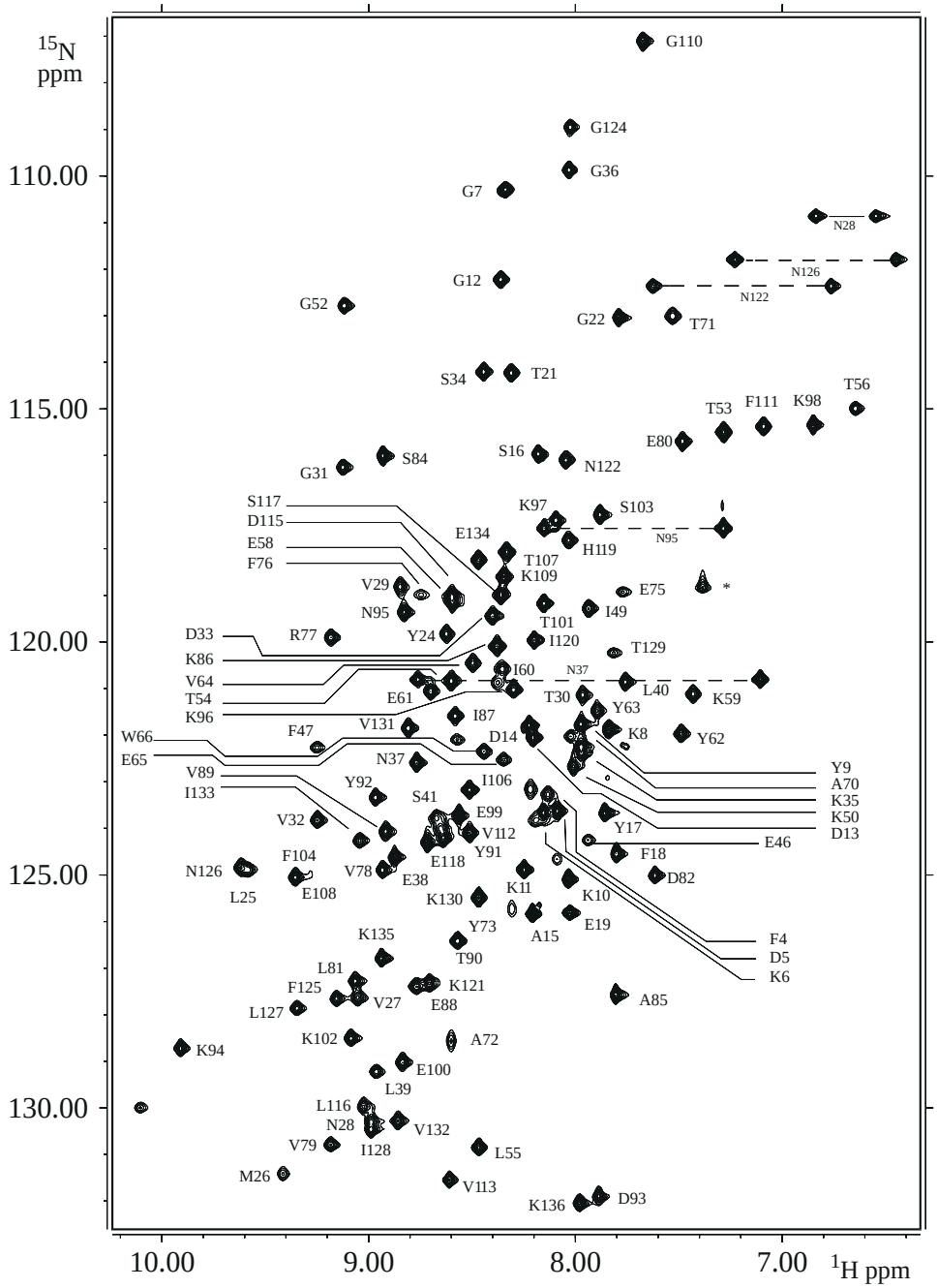

Fig. 1. ^{15}N-^{1}H HSQC spectrum of staphylokinase. The amide resonances are labelled with the one-letter code for amino acid type and sequence number. The asterisk indicates a folded peak. Pairs of resonances corresponding to asparagine side-chain amides are connected by dashed lines.

stretches: Pro–Tyr^{24}–Leu^{25}, Glu^{46}–Phe^{47}, Pro–Ile^{49}–Lys^{50}, Glu^{58}–Ile^{60}, Glu^{61}–Tyr^{63}, Val^{64}–Trp^{66}, Phe^{76}–Asp^{82}. This experiment also allowed complete assignment of the carbon resonances of most of the proline residues. Corresponding ^{1}H resonance assignments for proline residues were obtained from the HCCH-TOCSY experiment. At residues Gly^{7}, Asp^{13}, Met^{26}, Val^{27}, Asn^{28}, Val^{29}, Lys^{35}, Thr^{56}, Glu^{75}, Ile^{128}, the data from the scalar coupling based methods were supplemented by those from ^{15}N-edited HSQC-NOESY to achieve unambiguous linking of the fragments. The sequential assignments obtained from scalar coupling based methods were found to be consistent with the $H_i^{\alpha}H_{i+1}^{N}$ and $H^{N}{}_{i}H^{N}{}_{i+1}$ cross peaks seen in the NOE experiment (Figs. 4 and 5). Carbonyl resonance frequencies were obtained from the 3D HNCO spectrum. A summary of the connectivities used to obtain the sequential assignments is presented in Fig. 5. The chemical shift assignments are presented in Table 2. In the HSQC spectrum (Fig. 1), 11 of the amide NH peaks were very weak, presumably as a consequence of facile exchange with solvent water at pH 6.68 (lower pH could not be used due to aggregation). For these reson-

ances, the signal to noise ratio in the heteronuclear 3D experiments was poor. Consequently, there were seven residues (Ser[1], Ser[2], His[43] and Pro[42], Tyr[44], Ala[67], Leu[68]) for which unambiguous assignments were not yet obtained. For five residues (Ser[3], Val[45], Lys[57], Asp[69], Lys[74]), the NH assignments could not be deduced from the present data. As will be shown below, all of these residues lie outside the regions of secondary structure found for staphylokinase, which could be consistent with solvent exchange.

Secondary structure determination

Chemical shift index

After the sequential assignment was obtained, the consensus CSI of H^{α} (Wishart et al., 1992) and C^{α}, C^{β}, C' (Wishart and Sykes, 1994) was used to obtain a rough overview of the secondary structure elements from the NMR data. The $^{3}J_{H^{N}H^{\alpha}}$ coupling constants were screened to obtain further insight into the secondary structure elements. An upper threshold value of 5.5 Hz was taken

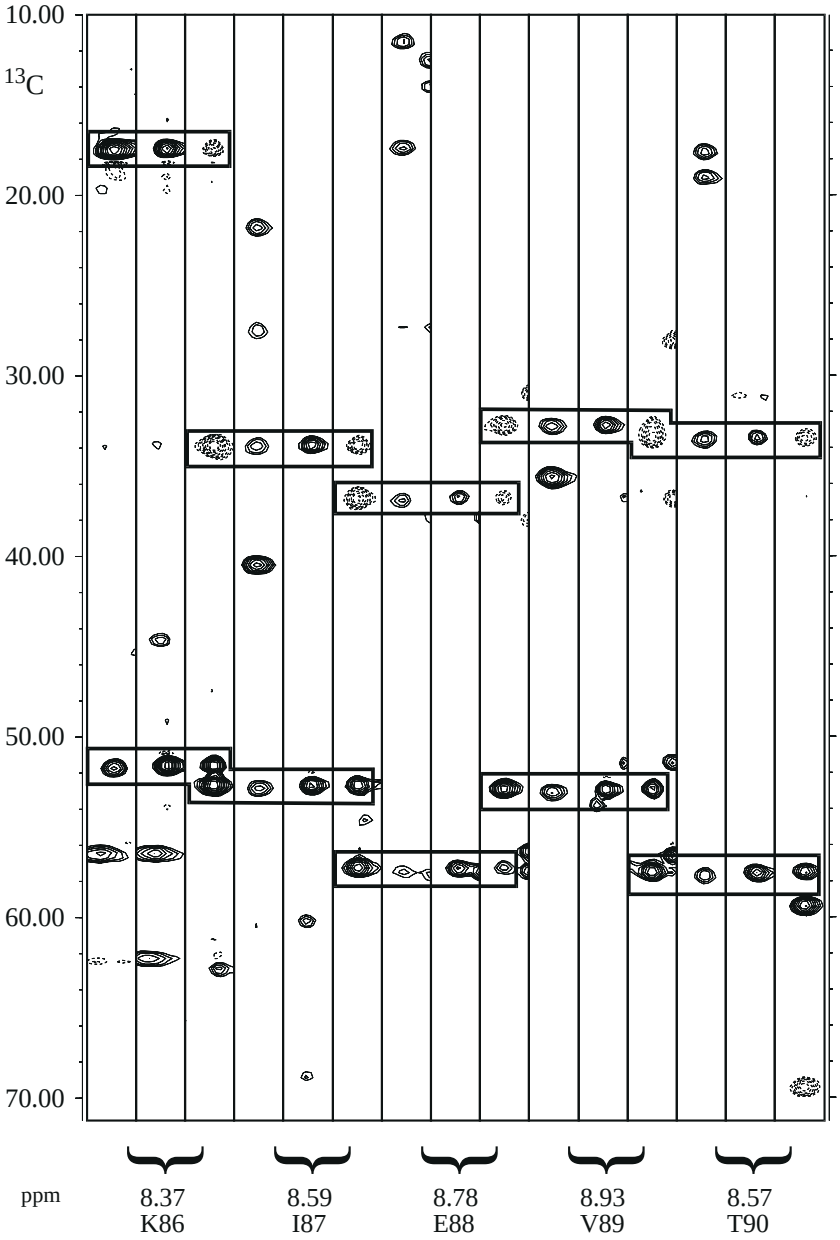

Fig. 2. Strip plots of the CC(CO)NH, CBCA(CO)NH and HNCACB spectra of Sak for the residues K86 to T90. For each residue a triple of strips (in the order given above) illustrates sequential assignments based on the $^{13}C^{\alpha}$ and $^{13}C^{\beta}$ chemical shifts and the amino acid type information obtainable from the CC(CO)NH spectrum. The slices have been taken at the ^{15}N frequency corresponding to the residue indicated. The boxes are drawn at the positions of the intra- and interresidual C^{α} and C^{β} resonances. In the HNCACB spectrum the interresidue cross peaks always have smaller intensities. The C^{β} resonances in this spectrum are of opposite sign and are indicated by dashed contours.

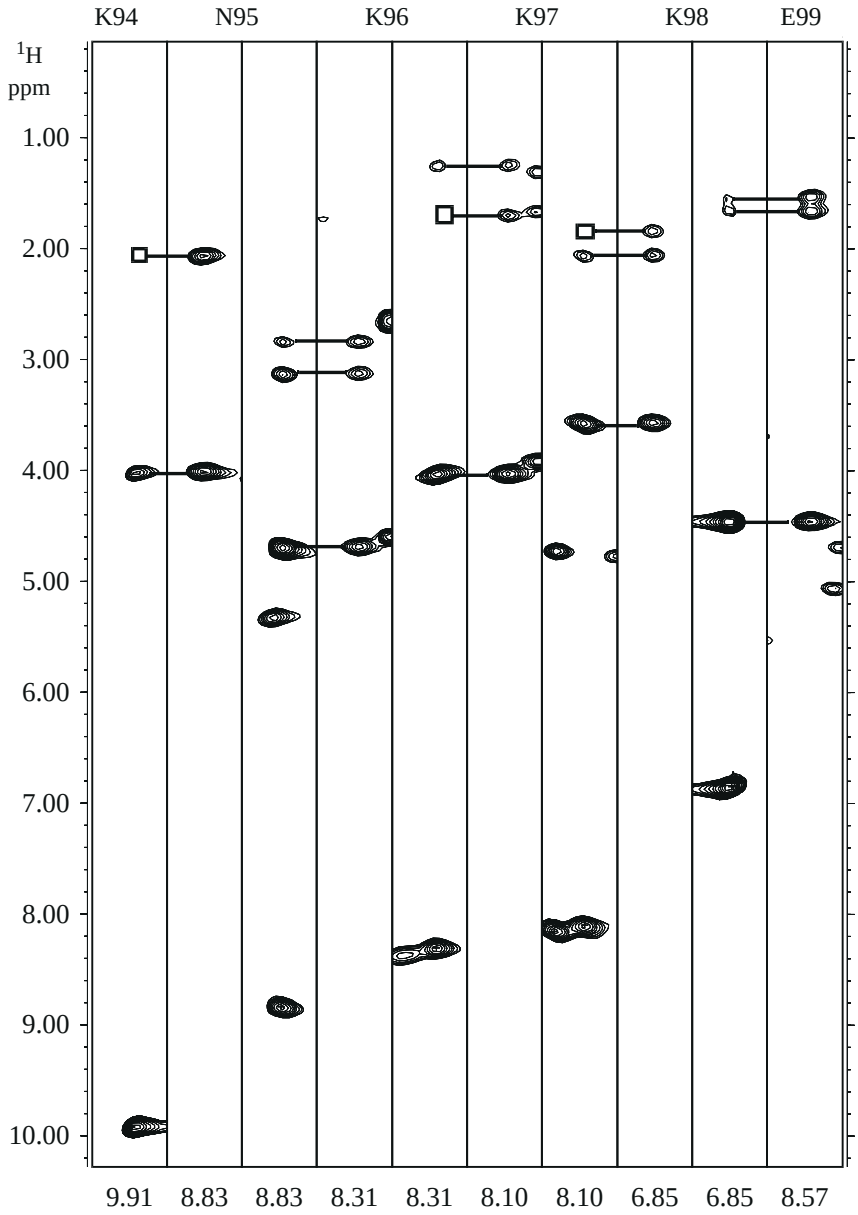

Fig. 3. Selected strips of the TOCSY-HSQC spectrum with intraresidual data and the HBHA(CBCACO)NH spectrum with interresidual data for Sak. The slices have been taken at the ^{15}N frequency corresponding to the residue indicated. Boxes show the positions of cross peaks which are observed at lower thresholds. The intra- and interresidual H^{α} and H^{β} peaks are indicated by bold lines. For residue 94 only the TOCSY-HSQC strip is given, and for residue 99 only the HBHA(CBCACO)NH strip is given.

to identify an α-helical ϕ-torsion angle and a lower limit of 7 Hz was used for a β-sheet (Pardi et al., 1984). Figure 5 also summarizes the results of the CSI method for staphylokinase, indicating six well-defined structural elements. The first 20 amino acids from the N-terminus show a 'random-coil' distribution. The only two glycines that have degenerate H^{α} chemical shifts are located in this stretch. A nine-residue stretch of β-sheet structure between Tyr[24] and Asp[33] (strand I) is predicted. After an irregular region, the consensus CSI predicts at least a three-residue β-strand for residues Thr[53]–Leu[55] (strand IV). Just prior to this region, a proline-rich sequence prevents a clean CSI pattern. Thus, for Val[45]–Ile[49] the prediction alternates between 'β-sheet' and 'irregular'. An α-helix starting at Gln[58] may consist of up to 12 residues. Since assignments for Ala[67] and Leu[68] have not been obtained so far, which would connect the helix to residues 59 and 60, the α-helix was at present restricted to residues 58–66. An irregular region then precedes a β-strand (VI) running from Lys[86] to Tyr[91]. β-strand VII consists of residues Lys[98]–Phe[104]. The C-terminus between Asn[126] and Glu[134] also exhibits a nine-residue β-strand (IX) element in the CSI index.

NOESY patterns for regular secondary structures

Because of the outstanding resolution of the amide NH

resonances observed for Sak (Fig. 1), the ^{1}H-^{15}N-^{1}H NOESY-HSQC and ^{15}N-^{15}N-^{1}H HSQC-NOESY-HSQC experiments provided a ready means to check for the existence of NOEs characteristic of α-helix and β-sheet regions of Sak.

α-Helix Typical NOEs observed for the α-helix are shown in Fig. 4. The observation of a complete set of strong N_iN_{i+1} NOEs for residues Glu[58]–Trp[66] is typical for distances of 2.6–2.8 Å in an α-helix. The helix type corresponds to a regular α-helix since weak α_iN_{i+4} NOEs were detectable, while a 3_{10}-helix would show no NOE effects due to a distance separation of 6.3 instead of 4.2 Å. The characteristic pattern starts at Glu[58] (α_i) and is observed up to Trp[66] (N_{i+4}). The absence of medium-sized α_iN_{i+2} cross peaks also excludes a 3_{10}-helix. The α-helix pattern was completed by a full set of α_iN_{i+1} and α_iN_{i+3} NOE cross peaks which could also be observed for Lys[57]. Seven of eight residues within this helix of 2.5 turns show J coupling constants less than 5.5 Hz, five of them even less than the 5 Hz expected for a helical ϕ-torsion angle of –60°. The formation of this α-helix places the polar and charged side chains of residues 58, 59, 61 and 65 on the same side of the helix surface.

β-Sheets A ^{15}N-edited NOESY-HSQC experiment detects exclusively NOEs originating at any proton and ending at an amide proton. This allows only partial infor-

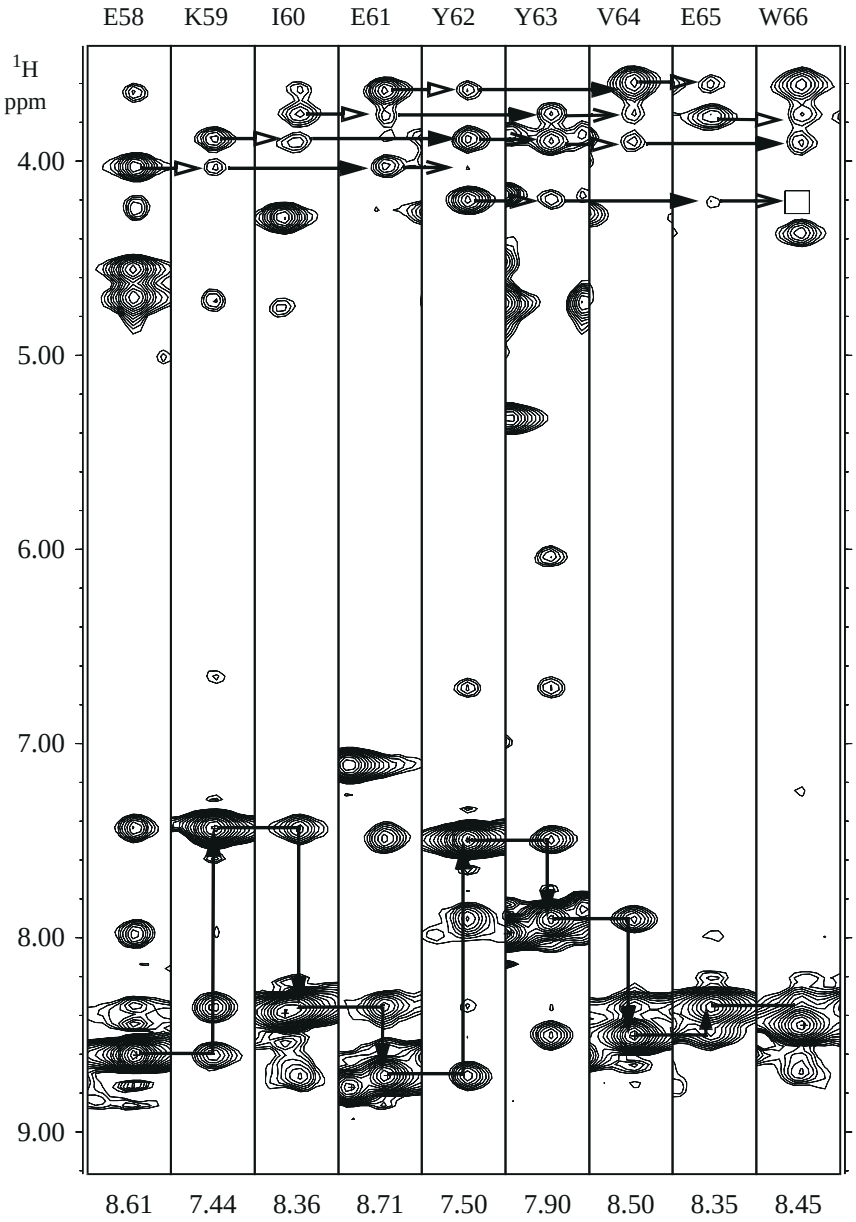

Fig. 4. Strip plots from the ^{15}N-edited NOESY-HSQC of Sak. The strips have been taken at the ^{15}N frequency corresponding to the residue indicated. $d_{H^NH^N}(i,i+1)$ connectivities are indicated by lines near 8 ppm. $d_{H^\alpha H^N}(i,i+1)$, $d_{H^\alpha H^N}(i,i+3)$ and $d_{H^\alpha H^N}(i,i+4)$ NOE connectivities typical for an α-helix are indicated by hollow, filled and stick arrows in the H^α region near 4 ppm, respectively.

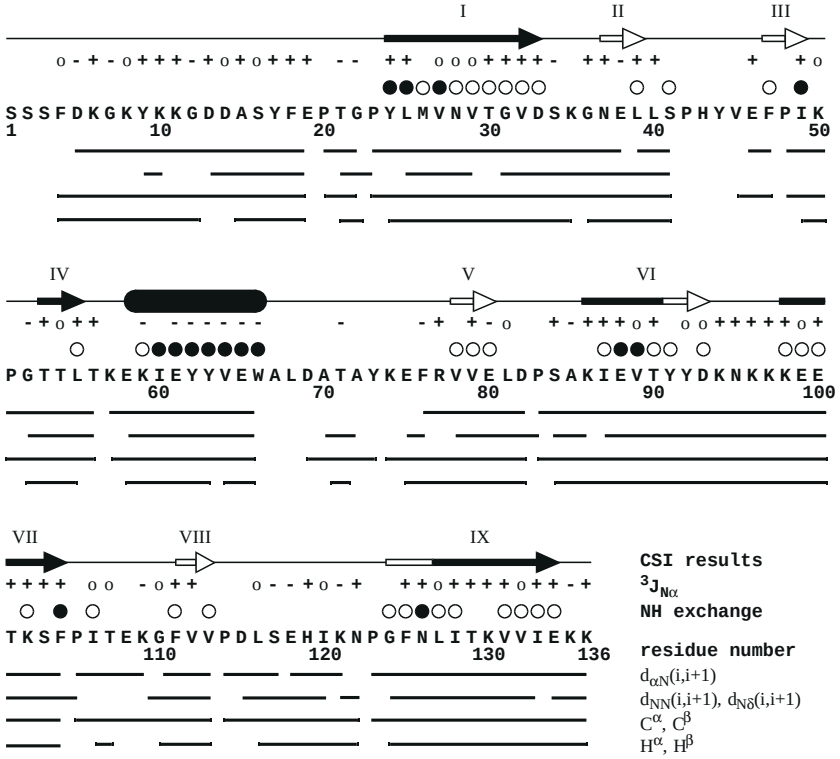

Fig. 5. Summary of NMR data characterizing sequential and secondary structure elements of Sak. Below the sequence are shown sequential connectivities obtained from ^{15}N-edited NOESY data ($d_{\alpha N}(i,i+1)$, $d_{NN}(i,i+1)$), from CC(CO)NH, CBCA(CO)NH and HNCACB experiments (C^α, C^β), and from TOCSY-HSQC and HBHA(CBCACO)HN experiments (H^α, H^β). For proline residues in position i+1 the $d_{N\delta}(i,i+1)$ connectivities are given. Above the sequence, an α-helical region is indicated by a tube and β-sheet regions are indicated by arrows, where open symbols indicate secondary structure detected in NOESY data and filled arrows indicate secondary structure identified by the consensus CSI (C', C^α, H^α and C^β CSI) and confirmed by NOESY data. The $^3J_{H^NH^\alpha}$ data are classified by '–' for $J < 5.5$ Hz, 'o' for $5.5 < J < 7$ Hz and '+' for $J > 7$ Hz. The rates observed for the H/D exchange of amide H^N hydrogens with solvent water are indicated by filled circles for slow (>48 h) exchange and open circles for medium ($1\ h < t < 48\ h$) exchange.

mation on the type of the β-sheets because H^α-H^α NOEs typical for antiparallel sheets will not be detected. Since, in addition, a few H^N-H^N signals with almost degenerate shifts were encountered in Sak, HSQC-NOESY-HSQC data were also analyzed. With the presently recorded experimental data, good NOESY evidence for the β-sheet regions of Sak was obtained primarily by the detection of H^N-H^N NOEs between two adjacent strands of β-sheet. The β-sheets observed in Sak are shown in Fig. 6. For residues Lys^{86}–Asp^{93} and Lys^{98}–Phe^{104}, an NOE network was revealed which is indicative of antiparallel β-strands. The ^{15}N-^1H-^1H HNHA experiment showed large $^3J_{H^NH^\alpha}$ coupling constants for residues Lys^{86}, Ile^{87}, Glu^{88} and Thr^{90} and for Glu^{100}–Phe^{104} (Fig. 5), which would also be consistent with the β-sheet conformation of strands VI and VII. The interaction of these two strands is terminated by Pro^{105}. From the H^N resonances of Lys^{86}, Glu^{88} and Thr^{90}, NOEs were observed to the H^N resonances of Gly^{124}, Asn^{126} and Ile^{128} (Fig. 6) and large $^3J_{H^NH^\alpha}$ coupling constants could be detected amongst residues 125–128 (Fig. 5), which would be consistent with an antiparallel β-sheet between strands VI and IX. Pro^{123} terminates the interaction of these two strands. Finally, the H^N resonances of Phe^{125} and Asn^{127} show NOEs to the H^N resonances of Tyr^{24}, Met^{26} and Asn^{28} and large $^3J_{H^NH^\alpha}$ coupling constants could be detected for residues 24 and 25, which is consistent with a parallel β-sheet between strands I and IX (Fig. 6). The start of this β-sheet is delineated by Pro^{23} and Pro^{123}. Throughout these β-sheet regions, intrastrand and interstrand H^N-H^α NOEs at the appropriate H^α chemical shifts could also be detected. This is further support for the β-sheet conformations, although the final confirmation of the H^α assignments of these cross peaks must await ^{13}C-edited NOESY data.

Similar data could be obtained for a variety of other regions of the sequence of Sak, leading to the overall secondary structure depicted in Fig. 7. In addition to the data discussed above, it is seen that the parallel β-sheet between strands I and IX is quite long and extends from Tyr^{24} to Asp^{33} and from Gly^{124} to Ile^{133}. Four further short sequences with NOEs characteristic of a β-strand were found. Strand IX (residues 124–134) not only forms a β-sheet with strand VI (residues 86–90), but also a β-sheet with strand V (residues 78–80). Between residues 81 and 85 there appears to be a bulge region centered on Pro^{83} (Fig. 7). A similar arrangement is observed for β-sheet

TABLE 2
^{15}N, ^{13}C AND ^{1}H RESONANCE ASSIGNMENTS (ppm) FOR STAPHYLOKINASE

Residue	N	H^N	C'	C^α	$H^\alpha/H^{\alpha1}/H^{\alpha2}$	C^β	$H^{\beta2}/H^{\beta3}$	Others
Ser[1]								
Ser[2]								
Ser[3]			172.8	56.8	4.37	61.2	3.76, 3.76	
Phe[4]	123.35	8.13	173.8	55.9	4.57	37.6	3.08, 2.94	
Asp[5]	123.58	8.10	174.7	52.3	4.53	38.7	2.69, 2.63	
Lys[6]	123.58	8.16	175.8	55.1	4.15	30.5	1.83, 1.74	C^γ 22.8; C^δ 26.9; C^ε 40.3; H^γ 1.39, 1.39
Gly[7]	110.32	8.35	172.7	43.6	3.87, 3.87			
Lys[8]	121.85	7.85	174.6	54.5	4.20	31.0	1.60, 1.60	C^γ 22.5; C^δ 27.2; C^ε 40.3; H^γ 1.18, 1.18
Tyr[9]	121.78	7.99	173.8	55.6	4.48	36.8	2.98, 2.82	
Lys[10]	125.16	8.05	174.2	54.0	4.25	31.3	1.62, 1.62	C^γ 22.5; C^δ 27.2; C^ε 40.3; H^γ 1.27, 1.27
Lys[11]	124.92	8.26	175.5	54.5	4.20	31.0	1.75, 1.69	C^γ 22.8; C^δ 27.2; C^ε 40.0; H^γ 1.37, 1.37
Gly[12]	112.25	8.36	172.4	43.3	3.92, 3.92			
Asp[13]	122.06	8.22	174.6	52.6	4.57	38.7	2.63, 2.63	
Asp[14]	121.81	8.23	174.6	52.7	4.55	38.7	2.68, 2.68	
Ala[15]	125.89	8.21	176.3	51.0	4.25	17.1	1.37	
Ser[16]	116.02	8.18	172.4	56.7	4.34	61.4	3.78, 3.78	
Tyr[17]	123.69	7.87	173.3	56.2	4.43	37.0	2.86, 2.86	
Phe[18]	124.55	7.82	172.7	55.1	4.51	38.1	2.98, 2.84	
Glu[19]	125.89	8.02		52.0	4.39	28.3	1.83, 1.83	H^γ 2.23, 2.23
Pro[20]			175.6	61.2	4.34	30.5	2.10, 1.84	C^γ 25.3; C^δ 48.9
								H^γ 1.63, 1.45; H^δ 3.58, 3.30
Thr[21]	114.35	8.30	172.9	59.7	4.34	68.5		
Gly[22]	113.11	7.81		43.0	4.58, 4.22			
Pro[23]			174.5	60.9	4.98	30.2	2.23, 2.23	C^γ 25.8; C^δ 47.4
								H^γ 2.30, 1.98; H^δ 3.92, 3.88
Tyr[24]	119.82	8.63	170.1	53.7	5.40	38.7	2.91, 2.95	
Leu[25]	124.91	9.61		50.9	5.32	43.6	1.74, 1.74	
Met[26]	131.40	9.41	172.6	52.9	5.07	31.4	2.09, 1.94	
Val[27]	127.72	9.07	171.1	60.3	4.58	31.3	2.30	C^γ 25.4, 21.7; H^γ 1.03, 1.03
Asn[28]	130.30	9.00	173.2	49.9	5.37	40.4	2.98, 2.98	N^δ 110.76; H^δ 6.84, 6.54
Val[29]	118.82	8.85	173.5	56.7	5.37	32.9	1.95	C^γ 19.8, 17.3
Thr[30]	121.21	7.97	172.4	60.0	4.43	69.7	3.87	C^γ 18.7; H^γ 1.18
Gly[31]	116.29	9.13	170.9	43.3	5.07, 3.14			
Val[32]	123.83	9.26	172.6	56.2	5.37	33.7	1.97	C^γ 19.5, 16.7
Asp[33]	119.58	8.40	177.7	50.2	5.28	40.4	3.49, 2.76	
Ser[34]	114.33	8.45	172.7	58.9	4.08	61.4	3.89, 3.89	
Lys[35]	122.39	7.97	175.3	53.4	4.47	30.7	2.04, 1.79	C^γ 23.1; C^δ 26.6; C^ε40.3
								H^γ 1.41, 1.41
Gly[36]	109.94	8.05	173.0	43.3	4.27, 3.45			
Asn[37]	122.59	8.77	173.5	51.2	4.55	36.8	2.79, 2.56	N^δ 120.78; H^δ 8.78, 7.11
Glu[38]	124.67	8.88	174.2	56.4	4.11	28.0	1.90, 1.90	C^γ 34.8
Leu[39]	129.30	8.96	174.8	53.4	4.48	43.0	1.20, 1.11	C^γ 25.0; C^δ 23.6, 20.9
Leu[40]	120.87	7.77	173.3	52.6	4.53	43.9	1.22, 1.03	C^γ 25.0; C^δ 23.6, 22.5
Ser[41]	124.01	8.66		53.9	4.86	60.7		
Pro[42]								
His[43]								
Tyr[44]								
Val[45]			171.5	59.2	4.20	33.7	1.78	C^γ 20.1, 19.9
Glu[46]	124.12	7.95	174.0	66.6	5.41	33.7	1.85, 1.85	C^γ 52.1
Phe[47]	122.22	9.25		52.5	5.00	40.0	2.95, 2.30	
Pro[48]			175.0	61.6	4.70	29.1	2.39, 1.95	C^γ 26.1; C^δ 49.3
								H^γ 2.30, 2.05; H^δ 3.94, 3.80
Ile[49]	119.30	7.94	172.2	57.2	4.69	40.9	1.53	C^γ 23.5, 15.7; C^δ 23.8
Lys[50]	122.77	8.01			4.88		1.69, 1.53	H^γ 1.44, 1.44
Pro[51]			175.2		3.97		2.02, 1.89	
Gly[52]	112.87	9.13	172.9	43.3	4.29, 3.43			
Thr[53]	115.66	7.29	171.3	60.0	4.27	68.5	3.99	C^γ 19.5
Thr[54]	120.91	8.60	173.0	60.0	4.67	66.3	3.90	C^γ 19.5; H^γ 0.90
Leu[55]	130.89	8.48	173.3	51.8	4.34	39.8	0.80, 0.80	C^γ 24.5; C^δ 22.5, 22.3
Thr[56]	114.99	6.66		57.7	4.27	69.9	4.71	

TABLE 2 (continued)

Residue	N	H^N	C'	C^α	$H^\alpha/H^{\alpha1}/H^{\alpha2}$	C^β	$H^{\beta2}/H^{\beta3}$	Others
Lys^{57}			173.0	58.9	3.66	30.8	1.71, 1.34	C^γ 22.3; C^δ 28.7; C^ϵ 40.0
Glu^{58}	119.11	8.60	177.2	57.5	4.04	27.7	1.98, 1.78	C^γ 34.3
Lys^{59}	121.15	7.45	176.6	56.4	3.90	30.7	1.76, 1.76	C^γ 22.9; C^ϵ 40.0
Ile^{60}	120.57	8.35	176.2	62.5	3.78	34.3	2.07	C^γ 27.3, 16.5; C^δ 18.9
Glu^{61}	121.08	8.70	177.1	58.9	3.64	26.9	2.17, 1.87	C^γ 35.9
Tyr^{62}	121.98	7.50	176.0	59.2	4.22	34.8	2.83, 1.55	
Tyr^{63}	121.51	7.90	176.8	59.2	3.92	35.4	2.79, 2.60	
Val^{64}	120.53	8.50	175.6	65.2	3.59	29.1	2.23	C^γ 21.4, 20.6
Glu^{65}	122.61	8.34	176.8	58.6	3.78	27.5	2.14, 2.14	C^γ 35.4
Trp^{66}	122.36	8.45		58.5	4.39	27.5		
Ala^{67}								
Leu^{68}								
Asp^{69}			175.9	52.3	4.59	38.7	2.68, 2.68	
Ala^{70}	122.06	8.03	177.1	51.8	4.15	16.5	1.44	
Thr^{71}	113.11	7.55	172.3	61.7	4.34	68.5	4.08	H^γ 1.13
Ala^{72}	128.49	8.61	174.7	52.6	4.58	17.3	1.39	
Tyr^{73}	125.66	8.30			4.45			
Lys^{74}			174.1	55.3	3.96		1.58, 1.58	C^γ 22.5; C^δ 28.3; C^ϵ 40.3
Glu^{75}	118.98	7.79	175.4	55.9	4.11	30.5	1.53, 1.53	C^γ 34.3
Phe^{76}	119.04	8.74	172.3	55.1	5.25	41.4	2.88, 2.88	
Arg^{77}	120.04	9.19	173.8	51.2	4.81	31.8	1.76, 1.62	C^γ 25.0; C^δ 41.4
Val^{78}	124.92	8.94	174.0	62.2	3.73	30.2	2.04	C^γ 20.9, 18.4
Val^{79}	130.82	9.19	174.8	62.5	3.94	30.5	1.69	C^γ 19.2, 18.7
Glu^{80}	115.71	7.50	173.0	54.0	4.55	30.7	2.12, 1.95	C^γ 33.2
Leu^{81}	127.23	9.07	174.4	52.9	4.41	40.9	1.60, 1.60	C^γ 26.1; C^δ 23.8, 23.4
Asp^{82}	125.12	7.63		51.2	4.67	41.2		
Pro^{83}			176.1	62.7	4.47	30.2	2.41, 2.02	C^γ 25.3; C^δ 49.6
								H^γ 1.93, 1.93; H^δ 3.95, 3.79
Ser^{84}	116.15	8.94	173.0	56.7	4.48	62.7	3.99, 3.95	
Ala^{85}	127.56	7.80	174.8	51.5	4.29	17.3	1.53	
Lys^{86}	120.10	8.37	172.7	52.6	4.79	34.0	1.76, 1.62	C^γ 21.7; C^δ 27.5; C^ϵ 40.3
Ile^{87}	121.66	8.59	174.0	57.3	5.04	36.8	1.88	C^γ 27.2, 17.3; C^δ 11.3
								H^γ 1.04
Glu^{88}	127.48	8.78	173.0	52.9	5.65	32.7	1.95, 1.95	C^γ 35.4; H^γ 2.19, 2.19
Val^{89}	124.19	8.93	170.4	57.5	4.81	33.5	1.29	C^γ 19.0, 17.6
Thr^{90}	126.44	8.57	171.7	59.2	5.54	69.3	3.71	C^γ 19.3; H^γ 1.01
Tyr^{91}	124.19	8.66	169.9	53.7	4.86	38.4	2.98, 2.73	
Tyr^{92}	123.33	8.96	172.4	56.4	4.29	36.5	3.01, 2.86	
Asp^{93}	131.85	7.91	175.0	50.4	4.53	40.5	2.72, 1.90	
Lys^{94}	128.75	9.91	176.1	56.7	4.04	30.7	2.09	C^γ 23.4; C^δ 27.5; C^ϵ 40.3
Asn^{95}	119.40	8.84	175.5	53.4	4.69	36.8	3.15, 2.84	N^δ 117.44; H^δ 8.16, 7.29
Lys^{96}	121.02	8.31	174.5	54.8	4.04	32.1	1.69, 1.27	C^γ 23.6; C^δ 27.5; C^ϵ 40.0
Lys^{97}	117.51	8.10	173.3	55.1	3.59	27.5	2.07, 1.85	C^γ 23.1; C^δ 26.4; C^ϵ 40.6
Lys^{98}	115.43	6.87	172.6	52.6	4.46	33.7	1.67, 1.55	C^γ 20.9; C^δ 27.2; C^ϵ 39.8
								H^γ 1.14, 1.14
Glu^{99}	123.80	8.56	173.7	54.8	4.48	28.6	1.88, 1.76	C^γ 35.7
Glu^{100}	129.06	8.84	172.5	52.6	4.51	31.3	1.32, 1.06	C^γ 33.5; H^γ 1.88, 1.88
Thr^{101}	119.19	8.17	172.2	59.2	5.35	69.8	3.71	C^γ 19.0; H^γ 0.97
Lys^{102}	128.53	9.09	172.5	52.1	4.53	33.2	1.67, 1.51	C^γ 23.1; C^δ 26.9; C^ϵ 40.3
Ser^{103}	117.27	7.90	171.7	54.3	5.33	63.8	3.57, 3.45	
Phe^{104}	125.15	9.36		52.5	4.76	39.1	1.93, 1.87	
Pro^{105}			174.1	60.0	4.70	30.5	2.25, 1.92	C^γ 24.7; C^δ 48.5
								H^γ 2.07, 2.07; H^δ 3.75, 3.74
Ile^{106}	123.09	8.51	174.5	58.9	4.46	34.8	1.93	C^γ 25.8, 15.4; C^δ 11.6
								H^γ 0.78
Thr^{107}	118.15	8.34	173.6	56.7	4.90	71.2	4.60	H^γ 1.46
Glu^{108}	124.93	9.24	176.9	57.8	4.24	27.5	2.13, 2.13	C^γ 34.6
Lys^{109}	118.63	8.33	176.3	55.6	4.13	30.7	1.88, 1.88	C^γ 23.4; C^δ 27.0; C^ϵ 40.3
								H^γ 1.52, 1.52
Gly^{110}	107.14	7.69	170.4	43.3	4.22, 3.78			
Phe^{111}	115.41	7.11	170.7	52.3	5.07	39.8	3.14, 2.98	

TABLE 2 (continued)

Residue	N	H^N	C'	C^α	$H^\alpha/H^{\alpha1}/H^{\alpha2}$	C^β	$H^{\beta2}/H^{\beta3}$	Others
Val^{112}	124.12	8.52	174.8	59.2	4.06	30.2	1.81	C^γ 19.5, 19.1
Val^{113}	131.63	8.61		59.3	3.50	30.1		
Pro^{114}			175.0	60.5	4.58	30.7	2.44, 1.89	C^γ 24.7; C^δ 48.5
								H^γ 2.04, 2.04; H^δ 3.89, 3.85
Asp^{115}	119.10	8.60	175.3	51.0	4.71	38.6	3.08, 2.51	
Leu^{116}	130.03	9.02	176.2	51.9	4.65	39.8	1.46, 1.46	C^γ 24.5; C^δ 20.2, 19.6
Ser^{117}	118.92	8.38	173.9	60.3	4.19	61.7	4.04, 3.86	
Glu^{118}	124.31	8.72	174.6	56.7	3.92	27.5	1.69, 1.34	C^γ 33.7
His^{119}	117.84	8.05	175.1	54.8	4.79	31.8	3.64, 2.79	
Ile^{120}	120.04	8.21	171.7	57.3	4.58	37.8	2.19	C^γ 27.2, 13.8; C^δ12.4
Lys^{121}	127.33	8.70	174.5	56.2	4.11	31.0	1.83, 1.83	C^γ 23.1; C^δ26.9; C^ε 40.3
Asn^{122}	116.15	8.06		48.8	4.67	35.7	2.77, 2.28	N^δ 112.21; H^δ 7.64, 6.78
Pro^{123}			172.6	61.4	4.18	29.6	1.69, 1.42	C^γ 25.5
Gly^{124}	108.97	8.02	171.0	42.2	3.15, 2.72			
Phe^{125}	127.71	9.17	173.0	54.8	4.41	36.2	3.08, 2.49	
Asn^{126}	124.90	9.62	173.0	52.1	5.28	39.2	2.96, 2.54	N^δ 111.79; H^δ 7.23, 6.46
Leu^{127}	127.96	9.35	172.6	52.1	4.90	41.6	2.19, 2.19	C^γ 25.3; C^δ 21.7, 26.4
Ile^{128}	130.46	9.00	174.6	58.3	5.02	36.7	1.86	C^γ 15.4; C^δ 12.1; H^γ 0.90
Thr^{129}	120.29	7.83	170.7	58.4	4.88	67.1	4.05	C^γ 16.5; H^γ 0.83
Lys^{130}	125.49	8.48	174.3	53.7	5.35	32.9	1.83, 1.72	C^γ 23.6; C^δ 27.5; C^ε 40.0
								H^γ 1.30, 1.30; H^δ 1.58, 1.58
Val^{131}	121.89	8.82	171.9	57.5	4.62	33.5	1.83	C^γ 20.1, 19.3; H^γ 0.87, 0.87
Val^{132}	130.26	8.87	174.8	60.0	4.72	29.4	1.93	C^γ 18.7, 18.6
Ile^{133}	124.29	9.05	172.3	57.0	5.40	40.3	1.76	C^γ 22.3, 16.8; C^δ 11.6
Glu^{134}	118.29	8.48	173.4	52.1	4.79	31.8	1.90, 1.90	C^γ 33.7; H^γ 2.19, 2.19
Lys^{135}	126.75	8.93	174.8	55.3	4.18	30.7	1.81, 1.66	C^γ 23.1; C^δ 26.9; C^ε 40.0
Lys^{136}	132.10	7.99		57.0	3.90	31.7	1.65, 1.39	H^γ 1.18, 1.18

formation between strand I (residues 24–33) and strands II (residues 37–39) and III (residues 47–49) with a bulge region containing Pro^{42} (Fig. 7). Finally, NOEs characteristic for a β-sheet could be observed for strands IV (residues 53–55) and VIII (residues 111–113). Because strands II, III, IV, V and VIII appear to be very short, it cannot be presently excluded that these strand regions may be distorted. This might account for the fact that with the exception of strand IV, these regions were not detected by the CSI index and not all of the $^3J_{H^NH^\alpha}$ coupling constants were large (Fig. 5). Apart from the N-terminal sequence, there appear to be only three longer sequences with irregular structures: residues 67–77, 105–110 and 115–123.

Turns For some of the sequence fragments which are not helix or β-sheet, α_iN_{i+1} and N_iN_{i+1} as well as α_iN_{i+2} and N_iN_{i+2} NOEs indicated a turn-like NOE pattern. The locations of these turns from Lys^{94}–Lys^{97} and Ser^{34}–Gly^{36} correspond well to the observed locations of a β-sheet. For the β-turn Lys^{94}–Lys^{97}, a number of NOEs to one $H^{N\delta}$ of Asn^{95} suggest a fixed conformation of the side chain above this turn. The presence of $d_{H^\alpha H^N}(i,i+2)$ correlations would be consistent with a type-I geometry of this turn. The NOE patterns suggest that a further turn may exist between Lys^{116}–Ile^{120}.

H/D exchange experiment

To provide further confirmation for regions of regular structure in Sak, the exchange of amide H^N hydrogens with solvent water was measured at pH 6.68. Within 30 min after the H/D exchange was initiated, approximately 50% (67 residues) of the amide protons showed largely complete deuterium exchange, and after 24 h 100 residues showed largely complete exchange. The finding that the N-terminal region lacks defined secondary structure elements is in agreement with the observation that up to Pro^{23} all hydrogens are substantially exchanged prior to recording the first HSQC spectrum (Fig. 5). Of the 48 amide H^N hydrogens which showed moderate or slow exchange (Fig. 5), all but two residues, Ser^{41} and Ile^{106}, are included in the helix and β-sheet regions shown in Fig. 7. The patterns for fast and slow or moderate exchange are generally in close agreement with the observed secondary structures. For example, all the amide H^N groups in the sequence 87–92, except for Tyr^{92}, show moderate or slow exchange, which is consistent with strand VI being the middle strand of a three-stranded β-sheet and strand IX terminating at Pro^{123} (Fig. 6). Similarly, with the exception of Glu^{99}, the alternating fast and slow or moderate exchange for residues 98–104 is consistent with strand VII corresponding to an outside strand in a β-sheet. Since Ser^{41}, Val^{27} and Val^{29} all show slow or moderate exchange, it seems likely that the bulge region near Pro^{42} forms an irregular hydrogen-bonded structure with the middle portion of β-sheet strand I (Fig. 7). In contrast, neither Lys^{130} nor any of residues 81–85 show amides with slow

exchange, suggesting that the bulge region near Pro[83] is less well structured. The amide hydrogens which are most stable towards exchange with solvent water are concentrated in the α-helix and in the region where strands I, III, VI, VII and IX form a five-stranded β-sheet (Fig. 7), suggesting that these structural elements probably constitute the structural core of Sak.

Discussion

The secondary structure elements of staphylokinase, a molecule of great pharmaceutical interest, have been determined via heteronuclear NMR. Backbone chemical shifts of 95% of the residues were assigned. By application of the CSI method, five regions corresponding to β-sheets and one central α-helix were detected. Measurements of $^{3}J_{H^{N}H^{\alpha}}$ coupling constants, HSQC-NOESY data and H/D exchange confirmed these structural elements. Four further, rather short regions of β-sheet were found by a combination of the latter three types of data. That these short β-sheet regions were not unambiguously predicted by the CSIs is probably a consequence of their shortness and possibly of irregular sheet conformations, e.g. sheet III contains a proline residue. Since the residues preceding and following the β-strands have been assigned and do not show NOEs characteristic of a β-sheet, the boundaries of the β-strands are well defined. Because Lys[57], Ala[67] and Leu[68] were not fully assigned, determination of the exact boundaries of the α-helix will require further data.

A previous characterization of the conformational properties of staphylokinase by small-angle X-ray scattering, dynamic light scattering, circular dichroism (Damaschun et al., 1993) and an infrared study (Dornberger et al., 1996) suggested that staphylokinase exhibits an elongated shape consisting of two domains separated by a central helix with an α-helical content of around 18%, 20% of the molecule in turn-like conformations and 30% incorporated in β-sheets. The findings on content of regular secondary structure are roughly consistent with the NMR results (9% α, 37% β), taking into account the error margin of the applied method. The proposal that Sak consists of two more or less independent domains in a fashion reminiscent of calmodulin or troponin c (Da-

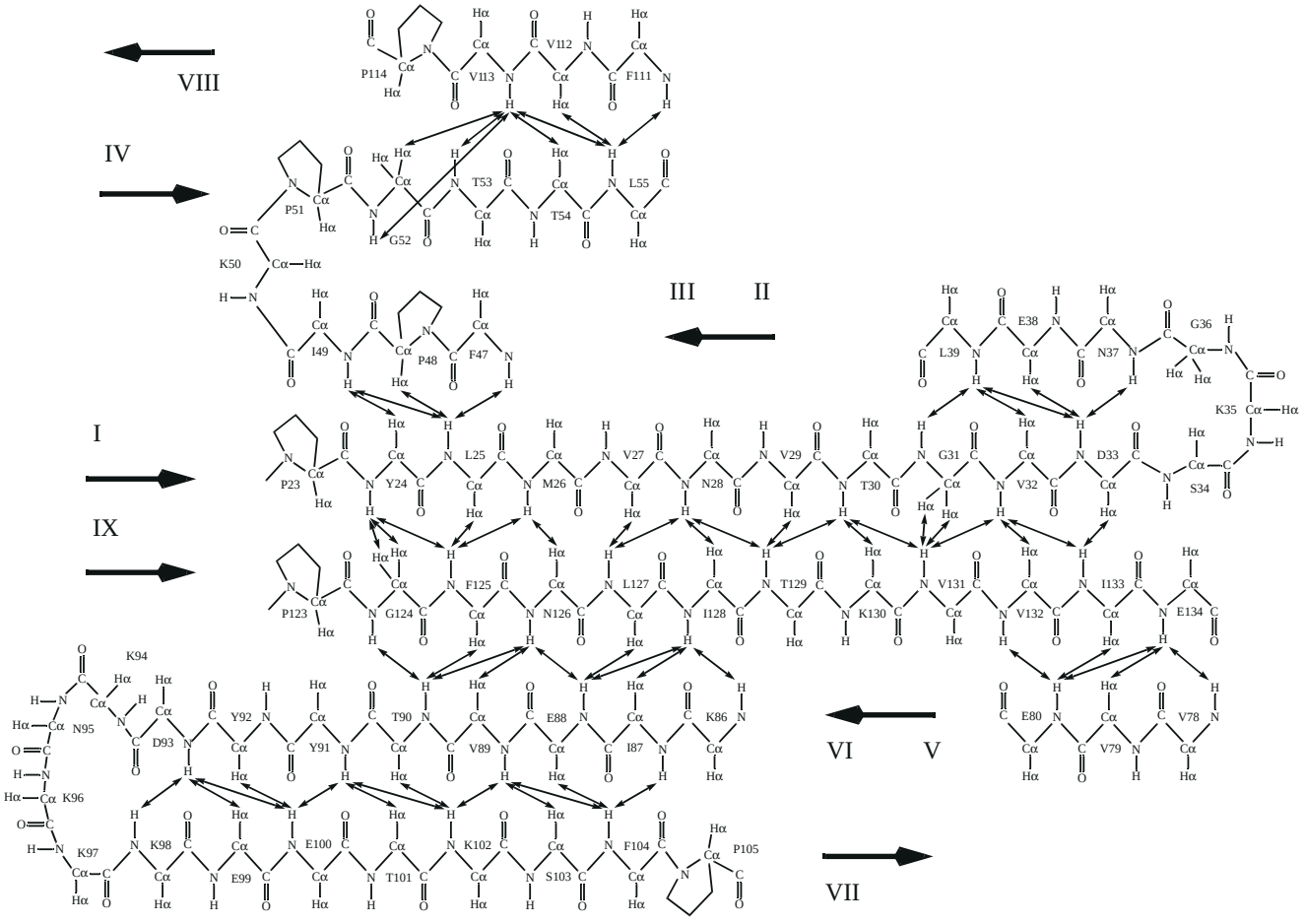

Fig. 6. The topology and NOE pattern observed for the nine strands of the β-sheets in Sak. Solid arrowheads indicate observed NOEs. The numbering and direction of the strands are also indicated.

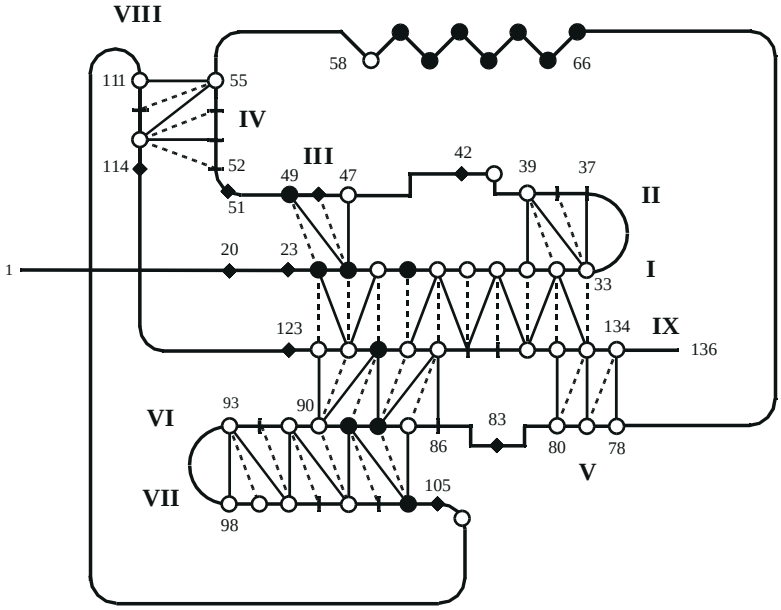

Fig. 7. Overall secondary structure and topology determined for Sak. For β-sheet regions, solid lines between strands indicate H^N-H^N NOEs and dashed lines between strands indicate H^N-H^α NOEs. Medium and slow exchange rates of amide H^N hydrogens with solvent are indicated by open and filled circles, respectively. Proline residues are indicated by filled diamonds.

maschun et al., 1993) is inconsistent with the secondary structure found in the present NMR experiments.

So far, three *sak* genes have been cloned from *Staphylococcus aureus* phages ϕC (Sako et al., 1983) and 42D (Behnke and Gerlach, 1987) as well as from chromosomal *Staphylococcus aureus* DNA (Collen et al., 1992). The three proteins Sakϕ C, Sak42D and SakSTAR, respectively, differ in only three amino acid positions, as schematically shown in Scheme 1. The sequence variation between the Sak species does not have any effect on the plasminogen activation potential of the proteins, although a difference in thermal stability of the variants was established and characterized in terms of thermal unfolding (Gase et al., 1994). These findings appear to be consistent with the present NMR secondary structure. The changes at residues 34 and 36 are located in a turn between antiparallel β-sheet strands (Fig. 7). Given the highly polar and charged nature of residues 33–37, this turn is almost certainly at the surface of the protein and the observed residue changes would not be expected to cause any major conformational changes in Sak. Similarly, the Arg^{43} to His^{43} exchange is relatively conservative and occurs in an irregular region of the secondary structure where such a change is apparently easily accommodated.

On the basis of the present NMR data, it appears that the first 10 residues have little role in determining the structure of Sak. During Plg activation, Sak is proteolytically processed by the removal of 10 amino acids from the N-terminus. This derivative, as well as a separately expressed Sak deletion mutant lacking the first 10 residues, has the same functional properties as the unprocessed Sak (Lijnen et al., 1992; Gase et al., 1996). Although these data indicate that residues 1–10 are not essential for the biological function of Sak, the N-terminal region must be easily accessible to the processing enzyme species, which is thought to be Pli. The lack of regular secondary structure elements found for the 20 N-terminal amino acids and the very fast H/D exchange observed for these residues suggest an irregular and possibly flexible conformation probably located at the surface of Sak, which would be consistent with the observed functional properties.

Several regions of Sak have been found to be important for the maintenance of functionality by means of mutational approaches. Mutagenesis of the unique methionine residue at position 26 of Sak revealed that only leucine and partly cysteine can replace methionine at this position without loss of plasminogen activator capability (Schlott et al., 1994a). This can now be understood in the sense that Met^{26} is located in the structural core of the protein and changes in this residue might be expected to cause substantial structural changes for Sak. In a more general approach for localizing regions of functional significance, clusters of charged amino acids were replaced by alanine residues (Silence et al., 1995). Of the 18 mutants generated, 15 showed only limited effects on the plasminogen activation properties of Sak and will not be

	NH_2	34	36		43	COOH
Sak42D	... D	G	K	R N E L L S P	R Y ...	
Sakϕ C		G	G		H	
SakSTAR		S	G		H	

Scheme 1. Alignment of proteins Sak42D, Sakϕ C and SakSTAR.

considered further here. The modification of three clusters within the amino acid sequence Lys^{11}–Asp^{14}, Glu^{46}–Lys^{50} and Glu^{65}–Asp^{69}, respectively, yielded Sak mutants for which the functional activity was almost completely lost (Silence et al., 1995). Modifications to residues 46–50 are located at the ends of β-sheet III and changes in residues 65–69 are at the C-terminal portion of the α-helix. The loss of functional activity for these mutants may reflect substantial conformational changes for Sak. Conversely, that mutations in structurally important regions at residues 26, 46–50 and 65–69 cause a loss of function suggests that the intact tertiary structure of Sak is important for interactions with plasminogen. In contrast, no evidence was obtained in the present work for an important structural role of residues 11–14. The mutational results therefore suggest that these residues may be important for the interaction of Sak with plasminogen, particularly since the mutants at residues 11–14 showed similar binding affinity to plasminogen, but reduced catalytic efficiency compared to wild-type Sak. In order to further understand the biological function, a full characterization of the 3D solution structure as well as the dynamical properties of staphylokinase is currently in progress in our laboratory.

Acknowledgements

The authors thank Mr. J. Leppert and Mr. M. Semm for continuous technical assistance. Furthermore, the excellent technical assistance of Ms. I. Tiroke in sample preparation is gratefully acknowledged. Support from the Fonds der Chemischen Industrie is also acknowledged.

References

Bartels, C., Xia, T., Billeter, M., Güntert, P. and Wüthrich, K. (1995) *J. Biomol. NMR*, **6**, 1–10.

Behnke, D. and Gerlach, D. (1987) *Mol. Gen. Genet.*, **210**, 528–534.

Bodenhausen, G. and Ruben, D.J. (1980) *Chem. Phys. Lett.*, **69**, 185–188.

Collen, D., Silence, K., Demarsin, E., De Mol, M. and Lijnen, H.R. (1992) *Fibrinolysis*, **6**, 203–213.

Collen, D., Schlott, B., Engelbourghs, Y., Van Hoef, B., Hartmann, M., Lijnen, H.R. and Behnke, D. (1993) *J. Biol. Chem.*, **268**, 8284–8289.

Collen, D. and Van de Werf, F. (1993) *Circulation*, **87**, 1850–1853.

Damaschun, G., Damaschun, H., Gast, K., Misselwitz, R., Zirwer, D., Gührs, K.-H., Hartmann, M., Schlott, B., Triebel, H. and Behnke, D. (1993) *Biochim. Biophys. Acta*, **1161**, 244–248.

Dornberger, U., Fandrei, D., Backmann, J., Hübner, W., Rahmelow, K., Gührs, K.-H., Hartmann, M., Schlott, B. and Fritzsche, H. (1996) *Biochim. Biophys. Acta*, **1294**, 168–176.

Fesik, S.W. and Zuiderweg, E.R.P. (1988) *J. Magn. Reson.*, **78**, 588–593.

Fujiwara, T., Anai, T., Kurihara, N. and Nagayama, K. (1993) *J. Magn. Reson.*, **A104**, 103–105.

Gase, A., Birch-Hirschfeld, E., Gührs, K.-H., Hartmann, M., Vettermann, S., Damaschun, G., Damaschun, H., Gast, K., Misselwitz, R., Zirwer, D., Collen, D. and Schlott, B. (1994) *Eur. J. Biochem.*, **223**, 303–308.

Gase, A., Hartmann, M., Gührs, K.-H., Röcker, A., Collen, D., Behnke, D. and Schlott, B. (1996) *Thromb. Haemostasis*, **76**, 755–760.

Grzesiek, S. and Bax, A. (1992) *J. Am. Chem. Soc.*, **114**, 6291–6293.

Grzesiek, S., Anglister, J. and Bax, A. (1993) *J. Magn. Reson.*, **B101**, 114–119.

Grzesiek, S. and Bax, A. (1993) *J. Biomol. NMR*, **3**, 185–204.

Kay, L.E., Ikura, M., Tschudin, R. and Bax, A. (1990) *J. Magn. Reson.*, **89**, 496–514.

Kay, L.E., Xu, G.Y., Singer, A.V., Muhandiram, D.R. and Kay, J.D.F. (1993) *J. Magn. Reson.*, **B101**, 333–337.

Lijnen, H.R., Van Hoef, B., De Cock, F., Okada, K., Ueshima, S., Matsuo, O. and Collen, D. (1991) *J. Biol. Chem.*, **266**, 11826–11832.

Lijnen, H.R., Van Hoef, B., Vandenbossche, L. and Collen, D. (1992) *Fibrinolysis*, **6**, 214–225.

Marion, D., Driscoll, P., Kay, L.E., Wingfield, P., Bax, A., Gronenborn, A.M. and Clore, G.M. (1989) *Biochemistry*, **28**, 6150–6156.

McCoy, M.A. and Müller, L. (1993) *J. Magn. Reson.*, **A101**, 122–130.

Pardi, A., Billeter, M. and Wüthrich, K. (1984) *J. Mol. Biol.*, **180**, 741–751.

Piotto, M., Saudek, V. and Sklenář, V. (1992) *J. Biomol. NMR*, **2**, 661–665.

Sako, T., Sawaki, S., Sakurai, T., Ito, S., Yosizawa, Y. and Kondo, I. (1983) *Mol. Gen. Genet.*, **190**, 271–277.

Schlott, B., Hartmann, M., Gührs, K.-H., Birch-Hirschfeld, E., Gase, A., Vettermann, S., Collen, D. and Lijnen, H.R. (1994a) *Biochim. Biophys. Acta*, **1204**, 235–242.

Schlott, B., Hartmann, M., Gührs, K.-H., Birch-Hirschfeld, E., Pohl, H.-D., Vanderschueren, S., Van de Werf, F., Michoel, A., Collen, D. and Behnke, D. (1994b) *Biotechnology*, **12**, 185–189.

Shaka, A.J., Barker, P.B. and Freeman, R. (1985) *J. Magn. Reson.*, **64**, 547–552.

Shaka, A.J., Lee, C.J. and Pines, A. (1988) *J. Magn. Reson.*, **77**, 274–293.

Silence, K., Collen, D. and Lijnen, H.R. (1993) *J. Biol. Chem.*, **268**, 9811–9816.

Silence, K., Hartmann, M., Gührs, K.-H., Gase, A., Schlott, B., Collen, D. and Lijnen, H.R. (1995) *J. Biol. Chem.*, **270**, 27192–27198.

States, D.J., Haberkorn, R.A. and Ruben, D.J. (1982) *J. Magn. Reson.*, **48**, 286–292.

Vanderschueren, S., Stockx, L., Wilms, G., Lacroix, H., Verhaeghe, R., Vermylen, J. and Collen, D. (1995) *Circulation*, **92**, 2050–2056.

Vuister, G.W. and Bax, A. (1993) *J. Am. Chem. Soc.*, **115**, 7772–7777.

Wishart, D.S., Sykes, B.D. and Richards, F.M. (1992) *Biochemistry*, **31**, 1647–1651.

Wishart, D.S. and Sykes, B.D. (1994) *J. Biomol. NMR*, **4**, 171–180.

Wittekind, M. and Müller, L. (1993) *J. Magn. Reson.*, **B101**, 201–205.

Zuiderweg, E.R.P. and Fesik, S.W. (1989) *Biochemistry*, **28**, 2387–2391.